Preprint No. ADP -00-54/T434

Regularization-independent study of renormalized non-perturbative quenched QED

Ayşe Kızılersü *, Tom Sizer † and Anthony G. Williams ‡

Special Research Centre for the Subatomic Structure of Matter and Department of Physics and Mathematical Physics, Adelaide University, 5005, Australia

Abstract

A recently proposed regularization-independent method is used for the first time to solve the renormalized fermion Schwinger-Dyson equation numerically in quenched QED_4. The Curtis-Pennington vertex is used to illustrate the technique and to facilitate comparison with previous calculations which used the alternative regularization schemes of modified ultraviolet cut-off and dimensional regularization. Our new results are in excellent numerical agreement with these, and so we can now conclude with confidence that there is no residual regularization dependence in these results. Moreover, from a computational point of view the regularization independent method has enormous advantages, since all integrals are absolutely convergent by construction, and so do not mix small and arbitrarily large momentum scales. We analytically predict power law behaviour in the asymptotic region, which is confirmed numerically with high precision. The successful demonstration of this efficient new technique opens the way for studies of unquenched QED to be undertaken in the near future.

*E-mail: akiziler@physics.adelaide.edu.au

†E-mail: tsizer@physics.adelaide.edu.au

‡E-mail: awilliam@physics.adelaide.edu.au

I. INTRODUCTION

The divergences inherent in quantum field theories have plagued physicists for years. The infinities are removed in a two-step process; first the divergences are controlled by a regulator, then the regulator is removed using the renormalization procedure to obtain finite, renormalization-independent physical quantities. Depending on the type of regulator introduced, different problems can occur. It is useful to discuss the difficulties that arise in the Schwinger-Dyson equations (SDE's) [1], since these are identical to the difficulties encountered in perturbation theory and because we will be using them as a tool to study non-perturbative QED. In the literature SDE's in quenched QED_4 are commonly studied by using the ultraviolet cut-off regularization scheme [2]. One difficulty faced is that the use of an ultra-violet (UV) cut-off Λ to regulate the integration will in general lead to an explicit violation of gauge covariance [3]. Because this regularization scheme does not respect translation invariance in the loop-momentum integration, it will lead to an explicit gauge-covariant violating contribution in the result, *even after* Λ is taken to infinity. More precisely, this violation of gauge invariance has been observed in quenched QED calculations employing the Curtis-Pennington (CP) [14] electron-photon vertex and may be traced back to a certain, logarithmically divergent, 4-dimensional momentum integral which vanishes because of rotational symmetry at all $\Lambda < \infty$, but leads to a finite contribution for $\Lambda \to \infty$. It is this discontinuous behaviour as a function of Λ which complicates correct numerical renormalization with this regulator. Incorrect results will be obtained unless care is taken to identify and remove 'gauge-covariance violating terms' [5]- [7]. In its favour, cut-off regularization is computationally economical compared to dimensional regularization, and gives accurate answers after gauge-covariant violating terms are removed.

On the other hand, SDE studies implemented using a gauge-invariant regularization scheme, such as dimensional regularization [8], will not have such a problem. However it will cause the generation of dynamical mass for all coupling constants in $D \neq 4$, instead of only above critical coupling in $D = 4$. In non-perturbative studies this scheme is computationally more demanding since a careful and time-consuming removal of the regulator must be performed involving an extrapolation of many high-precision solutions for different ϵ to $\epsilon = 0$. Additionally the accuracy of the results is, in practice, more limited because the integration range neccessarily extends to infinity.

In this paper we will be employing for the first time the regulator-independent method recently proposed by Kızılersü et.al. [9]. This method deals with the renormalized quantities only, as the regulator is removed analytically. The dependence on the mass scale introduced by the regulator is traded for the momentum scale μ at which the theory is renormalized *before* performing any numerical calculations. In this way dimensional regularization (or any other regulator which doesn't violate gauge covariance) can be used and the regulator removed analytically *before* any numerical calculations are begun. More importantly from a numerical pointof view, removal of the regulator means that no longer does one have to solve integral equations involving mass scales of vastly different orders of magnitude (and then, in addition, take a limit in which one of the scales goes to infinity). Rather, the important scales in the problem become scales of *physical* importance, such as the renormalized mass m_μ and the renormalization scale μ at which this mass is defined. It is therefore to be expected that the dominant contributions to any integrands will be from a finite region of

momenta. This feature is generic; i.e., it is independent of the particular vertex ansatz that one makes use of, and it remains a valid consideration for an arbitrary renormalizable field theory.

The regularization-independent approach is computationally very economical and very accurate; however the price paid is that one loses all contact with the bare theory. In particular, because of this, one cannot study dynamical chiral symmetry breaking in this approach by simply setting the bare mass $m_0 = 0$ and investigating at what value of coupling the dynamical fermion mass is generated. It is in this crucial point we differ from the analysis in Ref. [10] where, within quenched QED, a removal of the regulator was attempted in a manner which has some similarity to what we do here. Indeed, as emphasized by Miransky (Refs. [11], [12] as well as chapter 10.7 of Ref. [13]), some care needs to be taken with the treatment of the bare mass while removing the regulator in order to avoid drawing incorrect conclusions about the presence or absence of dynamical chiral symmetry breaking in gauge theories. In the present approach this problem is avoided. Dynamical chiral symmetry breaking, both explicit as well as dynamical, is characterized by a non-zero renormalized mass m_μ, and hence this quantity in itself cannot distinguish between these two possibilities. In section III A, we use (within quenched QED_4) the appearance of oscillations in the renormalized fermion mass function [11] as the indicator of the onset of dynamical symmetry breaking. All previous studies have confirmed that the occurrence of dynamical mass generation and UV oscillations coincide in quenched QED_4.

In this paper we demonstrate this approach numerically for the specific case of quenched QED_4 using the CP vertex to test its validity against previous works. Our goal is to ultimately implement this technique in studies of unquenched QED_4, which have now become numerically tractable because of this approach.

In section II we formulate the regularization-independent method for renormalized SDE for quenched QED in 4-dimensions with an arbitrary covariant gauge. Section III discusses the large momentum behaviour of the fermion propagator and gives its analytical form. We go on to solve SDE's numerically in Euclidean space for the fermion wave-function renormalization function and the mass function employing the CP vertex. The integration range in these equations is taken to infinity analytically and subsequently evaluated using a combination of numerical and analytic results. We do this extrapolation to infinity to facilitate comparison with previous results at very high momentum scales and to compare these results with their asymptotic forms. We demonstrate numerically to high precision the agreement between the regularization independent approach and the modified cut-off and dimensional regularization schemes. Finally, in section IV we summarize our results and conclude.

II. REGULARIZATION-FREE FORMALISM IN QUENCHED QED_4

The renormalized Schwinger-Dyson equation for the electron propagator (Fig. 1) can be formulated as

$$\begin{aligned} S^{-1}(\mu;p) &= Z_2(\mu){S^0}^{-1}(p) \;-\; iZ_1(\mu){e_0}^2 \int \frac{d^dk}{(2\pi)^d}\,\Gamma^\alpha(\mu;p,k)\,S(\mu;k)\gamma^\beta\,D^0_{\alpha\beta}(\mu;q)\,, \\ &\equiv Z_2(\mu){S^0}^{-1}(p) \;-\; iZ_1(\mu)\,\overline{\Sigma}(p) \quad . \end{aligned} \tag{2.1}$$

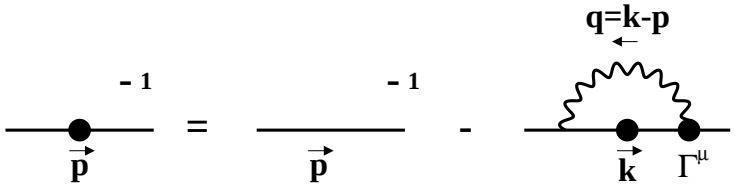

FIG. 1. The Schwinger-Dyson equation for the fermion propagator.

Here $Z_1(\mu)$ and $Z_2(\mu)$ are the vertex and fermion wave-function renormalization constants respectively. These renormalization constants relate the regularized but unrenormalized (i.e. *bare*) and renormalized propagator and vertex by

$$\Gamma_\mu(k,p\,;\mu) \;=\; Z_1(\mu,\Lambda)\,\Gamma^{\rm bare}_\mu(k,p\,;\Lambda) \quad , \tag{2.2}$$

$$S(p\,;\mu) \;=\; Z_2^{-1}(\mu,\Lambda)\,S^{\rm bare}(p\,;\Lambda) \quad . \tag{2.3}$$

In quenched QED, there is no renormalization of the electron charge ($e_0^2 = e_\mu^2 = 4\pi\alpha$) and the appropriate photon propagator is simply the tree-level form

$$D^0_{\alpha\beta}(q) \;=\; -\frac{1}{q^2}\left[\left(g_{\alpha\beta} - \frac{q_\alpha q_\beta}{q^2}\right) + \xi\frac{q_\alpha q_\beta}{q^2}\right] \quad , \tag{2.4}$$

where ξ is the covariant gauge parameter. We use $S(\mu;p)$ to denote the full fermion propagator renormalized at the momentum scale μ. It can be expressed in terms of two scalar functions, $Z(\mu^2;p^2)$, the fermion wave-function renormalization function, and $M(p^2)$, the mass function, by

$$S(\mu;p) \;=\; \frac{Z(\mu^2;p^2)}{\not{p} - M(p^2)} \quad . \tag{2.5}$$

Note that $S^0(p) \equiv 1/(\not{p} - m_0)$ is the tree-level fermion propagator (i.e., the bare fermion propagator in the absence of interactions). The full (proper) renormalized fermion-photon vertex is $\Gamma_\mu(\mu;k,p)$. Multiplying the fermion SDE Eq. (2.1) by $\not{p}$ and I and taking their respective spinor traces, we can separate the fermion self-energy $\overline{\Sigma}(p^2)$ into Dirac odd, $\overline{\Sigma}_d(p^2)$, and Dirac even, $\overline{\Sigma}_s(p^2)$, parts; i.e. $\overline{\Sigma}(p) = \not{p}\,\overline{\Sigma}_d(p^2) + \overline{\Sigma}_s(p^2)$. This gives

$$Z^{-1}(\mu^2;p^2) = Z_2(\mu) \;-\; Z_1(\mu)\,\overline{\Sigma}_d(p^2) \quad , \tag{2.6}$$

$$M(p^2)\,Z^{-1}(\mu^2;p^2) = Z_2(\mu)\,m_0 \;+\; Z_1(\mu)\,\overline{\Sigma}_s(p^2) \quad , \tag{2.7}$$

and these self energies make use of any regularization scheme which does not violate gauge covariance. Here, the bar over these quantities indicates that we have explicitly separated out the renormalization constants $Z_i(\mu)$; note that for notational brevity we do not indicate the implicit dependence on μ^2 of $\overline{\Sigma}_{d,s}(p^2)$ through the function $Z(\mu^2;p^2)$.

Because of the Ward-Takahashi identity, which must be satisfied by any acceptable vertex Ansatz for $\Gamma_\mu(\mu;k,p)$ and any acceptable renormalization scheme, one has $Z_1(\mu) = Z_2(\mu)$. Making use of this fact, Eqs. (2.6) and (2.7) can be rearranged as

$$Z_2^{-1}(\mu) = Z(\mu^2;p^2) - Z(\mu^2;p^2)\,\overline{\Sigma}_d(p^2) \quad , \tag{2.8}$$

$$M(p^2) \;=\; m_0 \;+\; \Big[M(p^2)\overline{\Sigma}_d(p^2) \;+\; \overline{\Sigma}_s(p^2)\Big] \quad . \tag{2.9}$$

In order to avoid cumbersome notation, we have not explicitly indicated functional dependence on the regulator in Eqs. (2.1)–(2.9) but it should be understood. The renormalization constants $Z_{1,2}(\mu)$ and the bare fermion mass m_0 are regulator dependent in the above equations. As one removes the regulator, the integrals on the right hand side of Eq. (2.1), and hence $\overline{\Sigma}_d(p^2)$ and $\overline{\Sigma}_s(p^2)$, diverge logarithmically. It is the defining feature of a renormalizable field theory that these divergences may be absorbed into the constants $Z_{1,2}(\mu)$ and into the bare mass m_0, rendering finite, regularization-independent limits for $Z(\mu^2;p^2)$ and $M(p^2)$. However, we can make use of the p^2 independence of $Z_{1,2}(\mu)$ and m_0 in order to eliminate these constants from the above equations. The renormalization conditions for the fermion wave-function renormalization function and the mass function are

$$Z(\mu^2;\mu^2) \;=\; 1 \qquad \text{and} \qquad M(\mu^2) \;\equiv\; m_\mu \quad . \tag{2.10}$$

Evaluating Eqs. (2.8) and (2.9) at a second momentum which, we take to be $p^2 = \mu^2$, and taking the difference one obtains the central equations that we solve here

$$\boxed{\begin{aligned} Z(\mu^2;p^2) \;&=\; 1 \;+\; Z(\mu^2;p^2)\,\overline{\Sigma}_d(p^2) \;-\; \overline{\Sigma}_d(\mu^2) \quad , \\ M(p^2) \;&=\; m_\mu \;+\; \Big[M(p^2)\overline{\Sigma}_d(p^2) \;+\; \overline{\Sigma}_s(p^2)\Big] \;-\; \Big[m_\mu\overline{\Sigma}_d(\mu^2) \;+\; \overline{\Sigma}_s(\mu^2)\Big] \;. \end{aligned}} \tag{2.11}$$

As the left hand sides of these equations must be finite as the regulator is removed, then the right hand side must be also, even though the individual terms on the RHS may *separately* diverge.

These renormalized equations Eq. (2.11) with the regulator removed provide a starting point for non-perturbative investigations which have significant advantages over the usual treatment found in the literature [2]- [8]. In the following section we shall illustrate this approach by turning to the example of quenched QED with the Curtis-Pennington vertex.

III. QUENCHED QED WITH THE CURTIS-PENNINGTON VERTEX

In this section we use the regulator-independent method for solving the renormalized SDE in Eq. (2.11) in an arbitrary covariant gauge. As usual we write the full vertex as a sum of the Ball-Chiu vertex [15] (longitudinal part satisfying the Ward-Takahashi identity) and the Curtis-Pennington term [14] (the transverse part satisfying multiplicative renormalizability of the fermion propagator),

$$\Gamma^\mu(\mu;k,p) = \Gamma^\mu_{BC}(\mu;k,p) + \tau_6(\mu;k,p)\,\Big[\gamma^\mu(p^2-k^2) + (p+k)^\mu(\not{k} - \not{p})\Big] \quad , \tag{3.1}$$

where $\Gamma^\mu_{BC}(\mu;k,p)$ and $\tau_6(\mu;k,p)$ are given in appendix A. After Wick rotating into Euclidean space and performing the angular integration, Eq. (2.11) can be written as

$$Z(\mu^2;p^2) = 1 - \frac{\alpha\xi}{4\,\pi}\int_{p^2}^{\mu^2} dk^2 \frac{1}{[k^2+M^2(k^2)]}\,Z(\mu^2;k^2) + \frac{\alpha}{4\,\pi}\int_0^{\infty}\frac{dk^2}{[k^2+M^2(k^2)]}\left[Z(\mu^2;p^2)\,I(k^2,p^2) \;-\; I(k^2,\mu^2)\right], \tag{3.2}$$

$$M(p^2) = m_\mu + \frac{\alpha}{4\pi}\int_0^{\infty}\frac{dk^2}{[k^2+M^2(k^2)]}\Big[J(k^2,p^2) - J(k^2,\mu^2) + M(p^2)\,I(k^2,p^2) - m_\mu\,I(k^2,\mu^2)\Big], \tag{3.3}$$

where the kernel functions $I(p^2,k^2)$ and $J(p^2,k^2)$ are also given in appendix A. The kernels have the same form as Ref. [16] except that the gauge-covariance violating term has been removed, since it does not survive the four-dimensional momentum integration in the absence of a cut-off. This term does not vanish if the angular integral is done first with the radial integral taken to infinity afterwards, which is why it must be removed by hand in the cut-off approach.

The above equations are finite which can be seen by analysis of the large momentum limits of the integrands for Z and M, which behave asymptotically as $(k^2)^{-n}$ and $(k^2)^{-r}$ respectively, where $n, r > 1$. The equation for the wave-function renormalization function Eq. (3.2) is the same as Eq. (10) in Ref. [10], however our treatment of the mass function differs from theirs.

A. Asymptotic limits of the solutions

In this subsection we solve Eqs. (3.2) and (3.3) analytically for momenta p^2 much larger than $M^2(p^2)$ (the asymptotic region) by linearizing them for finite mass, in a manner similar to that used by Atkinson et al. [16] for the chirally symmetric theory (i.e. $m_0 = 0$). It is convenient to *temporarily* take the renormalization point μ to also be very large, removing this constraint once our derivation is complete. The integrals in Eqs. (3.2) and (3.3) are dominated by contributions around $k^2 = p^2$ and $k^2 = \mu^2$, so when p^2 and μ^2 are in the asymptotic region k^2 is neccessarily also much greater than $M^2(k^2)$. Expanding in powers of $M^2(k^2)/k^2$ and keeping at most linear terms in $M(k^2)$, the kernel functions take their asymptotic forms $I(p^2,k^2) \to 0$ and $J(p^2,k^2) \to J'(p^2,k^2)$, where $J'(k^2;p^2)$ is defined in appendix A. Hence when p^2 and μ^2 are both in the asymptotic region, we obtain

$$Z(\mu^2;p^2) = 1 \;-\; \frac{\alpha\xi}{4\pi}\int_{p^2}^{\mu^2}\frac{dk^2}{k^2}Z(\mu^2;k^2) \quad , \tag{3.4}$$

$$M(p^2) = m_\mu \;+\; \frac{\alpha}{4\pi}\int_0^{\infty} dk^2\left[J'(k^2,p^2) - J'(k^2,\mu^2)\right] \quad . \tag{3.5}$$

These linearized equations are scale invariant and admit power law solutions.

The solution of this asymptotic form of the Z equation is easily seen to be [3]

$$Z(\mu^2;p^2) \;=\; \left(\frac{p^2}{\mu^2}\right)^{\nu} \qquad \text{with} \qquad \nu = \frac{\alpha\xi}{4\pi} \quad , \tag{3.6}$$

which differs from Ref. [16] due to the absence of the gauge covariance violating term. We thus obtain for p^2 and p'^2 both large that

$$\frac{Z(\mu^2;p^2)}{Z(\mu^2;p'^2)} \;=\; \left(\frac{p^2}{p'^2}\right)^{\nu} \qquad \text{with} \qquad \nu = \frac{\alpha\xi}{4\pi} \quad , \tag{3.7}$$

which is valid for an *arbitrary* renormalization point μ since the ratio is by definition renormalization-point independent. It then follows that for large p^2 and any arbitrary μ^2 that

$$Z(\mu^2;p^2) \;=\; C_\mu \left(\frac{p^2}{\mu^2}\right)^{\nu} \qquad \text{with} \qquad \nu = \frac{\alpha\xi}{4\pi} \quad , \tag{3.8}$$

for some appropriate C_μ such that $C_\mu \to 1$ as μ^2 enters the asymptotic region.

We shall see that power law solutions of the M equation occur in two regimes, depending on the value of α. Those with a real exponent can be identified with the subcritical regime, where α is less than its critical value α_c which marks the onset of dynamical chiral symmetry breaking. Those with complex exponent correspond to oscillating solutions which correspond to the supercritical regime where $\alpha > \alpha_c$. We examine these two cases separately in what follows.

1. Subcritical asymptotic solution

Where, as before, μ^2 and p^2 are understood to be chosen much greater than all other mass scales, we try a solution of Eq. (3.5) of the form

$$M(p^2) \;=\; m_\mu \left(\frac{p^2}{\mu^2}\right)^{-s}, \qquad s \in R\,. \tag{3.9}$$

Solving for s, we find

$$\frac{3\nu}{2\xi}\Bigg[2\pi\cot s\pi - \pi\cot\nu\pi + 3\pi\cot(\nu-s)\pi + \frac{2}{(1-s)} + \frac{1}{(\nu+1)} + \frac{1}{\nu} - \frac{3}{(\nu-s)} - \frac{1}{(\nu-s+1)}\Bigg] + \frac{s-1}{\nu-s+1} = 0 \quad . \tag{3.10}$$

This equation is the same as in Ref. [16], but in contrast to the unrenormalized equation examined in that paper, this power Ansatz is valid for the renormalized equation that we have here whether or not the bare mass m_0 is zero. We can again form a ratio, i.e., provided p^2 and p'^2 are much larger than all other mass scales then we have

$$\frac{M(p^2)}{M(p'^2)} \;=\; \left(\frac{p^2}{p'^2}\right)^{-s}, \qquad s \in R\,. \tag{3.11}$$

Both Eqs. (3.10) and (3.11) are manifestly renormalization-point independent and so are valid for an arbitrary choice of renormalization point μ. It then follows that for large p^2 and any arbitrary μ^2 that

$$M(p^2) \;=\; D_\mu \left(\frac{p^2}{\mu^2}\right)^{-s}, \qquad s, D_\mu \in R \tag{3.12}$$

for some appropriate D_μ. We see that $D_\mu/(\mu^2)^{-s}$ is a renormalization-point independent constant and that we must have $D_\mu \to m_\mu$ as μ^2 moves into the asymptotic region.

There is in fact more than one real solution to s in Eq. (3.10) (see also Ref. [16]), e.g., in Landau gauge there are two. However, only one of these matches smoothly onto the perturbative solution, and hence is the relevant solution. The other solutions appear as a spurious byproduct of the linearized approximation in Eq. (3.5) (Solutions which do not match smoothly onto perturbation theory can arise in Eq. (3.5) if the integrals diverge like $1/\alpha$, due to infrared divergences; this cannot occur in Eq. (3.3) because of the regulating mass in the denominator). Since s is real there are no oscillations in the mass function and hence there is no chiral symmetry breaking for these couplings. While Atkinson et. al. are unable to generate a mass in this region, due to their initial condition being $m_0 = 0$, we are able to do so since we are not confined by this constraint.

2. Supercritical asymptotic solution

In the case where s is complex, the (real) mass function is a superposition of powers of s and its complex conjugate. For large p^2 and arbitrary μ^2 we have as the counterpart to Eq. (3.12)

$$M(p^2) = \frac{1}{2} D_\mu \left(\frac{p^2}{\mu^2}\right)^{-s} + \frac{1}{2} D_\mu^* \left(\frac{p^2}{\mu^2}\right)^{-s^*}, \qquad s, D_\mu \in C \tag{3.13}$$

where D_μ is some appropriate complex constant, and

$$\frac{1}{2}\left(D_\mu + D_\mu^*\right) \;=\; \mathrm{Re}\left(D_\mu\right) \to m_\mu \tag{3.14}$$

as μ^2 enters the asymptotic region. Here s and s^* are complex conjugate solutions to Eq. (3.10) and the combination results in a mass function that oscillates. This oscillatory behaviour is more transparent if we write Eq. (3.13) as

$$M(p^2) = \left(\frac{p^2}{\mu^2}\right)^{-\mathrm{Re}\,(s)} \left\{ \mathrm{Re}\left(D_\mu\right) \cos\left[\mathrm{Im}\left(s\right) \log\left(p^2/\mu^2\right)\right] + \mathrm{Im}\left(D_\mu\right) \sin\left[\mathrm{Im}\left(s\right) \log\left(p^2/\mu^2\right)\right] \right\} \tag{3.15}$$

which has the form of a phase-shifted cosine function periodic in $\log(p^2/\mu^2)$, with a period of $2\,\pi/\mathrm{Im}\,(s)$, modulated by an exponentially decaying envelope of $(p^2/\mu^2)^{-\mathrm{Re}\,(s)}$. The oscillations are an indication that chiral symmetry is broken in quenched QED employing the CP vertex at sufficiently strong coupling $\alpha > \alpha_c$.

B. Numerical solutions

In the regularization-independent approach, the equations are constructed so as to remove all infinities from the outset and so the UV region of the integral is not a crucial

limiting factor. Moreover, establishing exact asymptotic forms of the wave-function renormalization and mass functions in the previous subsection make it possible to analytically integrate Eqs. (3.2) and (3.3) from the highest grid point to infinity. We denote this highest grid point, where the asymptotic analytic forms are matched onto the numerical results, as the "matching point" k_m^2. Hence we can rewrite Eqs. (3.2) and (3.3) as

$$\begin{aligned} Z(\mu^2;p^2) \equiv 1 &- \frac{\alpha\xi}{4\,\pi}\int_{p^2}^{\mu^2} dk^2 \frac{1}{[k^2+M^2(k^2)]}\,Z(\mu^2;k^2) \\ &+ \frac{\alpha}{4\,\pi}\int_0^{k_m^2} \frac{dk^2}{[k^2+M^2(k^2)]}\left[Z(\mu^2;p^2)\,I(k^2,p^2)\;-\;I(k^2,\mu^2)\right] \\ &+\; Z_{\rm high}(\mu^2;k_m^2,p^2), \qquad (3.16) \\ M(p^2) \equiv m_\mu &+ \frac{\alpha}{4\pi}\int_0^{k_m^2} \frac{dk^2}{[k^2+M^2(k^2)]}\left[J(k^2,p^2)-J(k^2,\mu^2)\right. \\ &\left.+\,M(p^2)\,I(k^2,p^2)-m_\mu\,I(k^2,\mu^2)\right] \;+\; M_{\rm high}(\mu^2;k_m^2,p^2)\;, \qquad (3.17) \end{aligned}$$

where the matching point, k_m^2, is chosen sufficiently large that the asymptotic formulas are valid ($k_m^2 \gg M^2(k_m^2)$). These equations serve as definitions of the analytic forms that we need to evaluate, i.e., $Z_{\rm high}(\mu^2;k_m^2,p^2)$ and $M_{\rm high}(\mu^2;k_m^2,p^2)$ are defined as the contributions arising from integrating from k_m^2 to infinity for Eqs. (3.16) and (3.17) respectively. The analytic forms for $Z_{\rm high}$ and $M_{\rm high}$ and their derivations are given in appendix B. By calculating $Z(\mu^2;p^2)$ and $M(p^2)$ in this way we can achieve very high accuracy in the UV region.

Eqs. (3.16) and (3.17) have been solved numerically in Euclidean space for $Z(\mu^2;p^2)$ and $M(p^2)$ with a variety of gauges ξ, renormalization points μ^2 and renormalized masses m_μ for the couplings $\alpha = 0.6$ (subcritical) and $\alpha = 1.5$ (supercritical). Each solution was iterated from an initial guess until $Z(\mu^2;p^2)$ and $M(p^2)$ converge; our convergence criteria is that the change in successive solutions is less than one part in 10^8 at each momentum point. Every iteration the data is refitted to the asymptotic analytic forms of $Z(\mu^2;p^2)$ and $M(p^2)$.

We have found, in line with the above discussion, that the regularization-independent method allows us to extend solutions for momenta up to 10^{65} as opposed to solutions obtained from cut-off regularization where numerical round-off error meant that the momenta in our solutions could typically not exceed $\mathcal{O}(10^{18})$ [2], [5], [7]. We also verified that our solutions do not change when we vary the location of the point k_m where the matching of our numerical and analytical solutions is carried out.

In Figs. 2 and 3, we show typical solutions, using regularization independent regularization, of the fermion wave-function renormalization and mass functions for subcritical ($\alpha = 0.6$) and supercritical ($\alpha = 1.5$) cases respectively. Also shown are corresponding solutions based on the theoretical asymptotic powers with fitted scales. The log-log nature of the figures emphasizes the UV behaviour of the propagator. One can see there is excellent agreement in the region $p^2 \gg M^2(p^2)$. To emphasize this point we present the theoretical and numerically calculated powers for these two solutions in Table I.

In summary : our knowledge of the exact forms of $Z(\mu^2;p^2)$ and $M(p^2)$ in the asymptotic region saves us from the need to extend our numerical solutions far into the ultra-violet. Therefore Eqs. (3.16) and (3.17) are solved numerically up to the matching point (k_m^2) in the UV, whereafter the analytical solution joins smoothly to the numerical one. The

fitting parameters $[C_\mu, \mathrm{Re}\,(D_\mu), \mathrm{Im}\,(D_\mu), \mathrm{Re}\,(s), \mathrm{Im}\,(s), \nu]$ for the analytic continuation are re-calculated after each iteration.

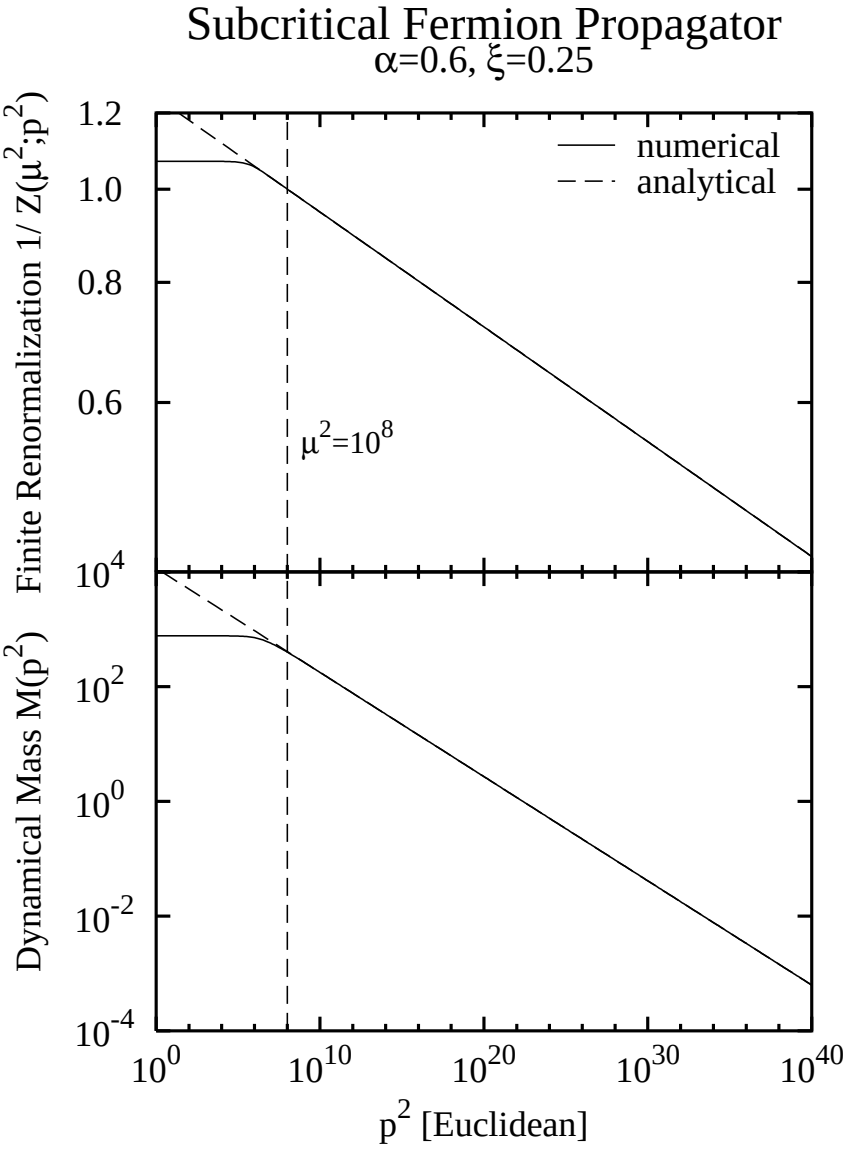

FIG. 2. Comparison of the numerical solution for the finite renormalization $1/Z(\mu^2; p^2)$, and the mass function $M(p^2)$ (solid lines) and their predicted asymptotic behaviour with matching scales (dashed lines) from Eqs. (3.8) and (3.12) for the subcritical coupling $\alpha = 0.6$. The example solution was for a renormalized mass $m_\mu = 400$ (arbitrary units), renormalization point $\mu^2 = 10^8$ and gauge parameter $\xi = 0.25$.

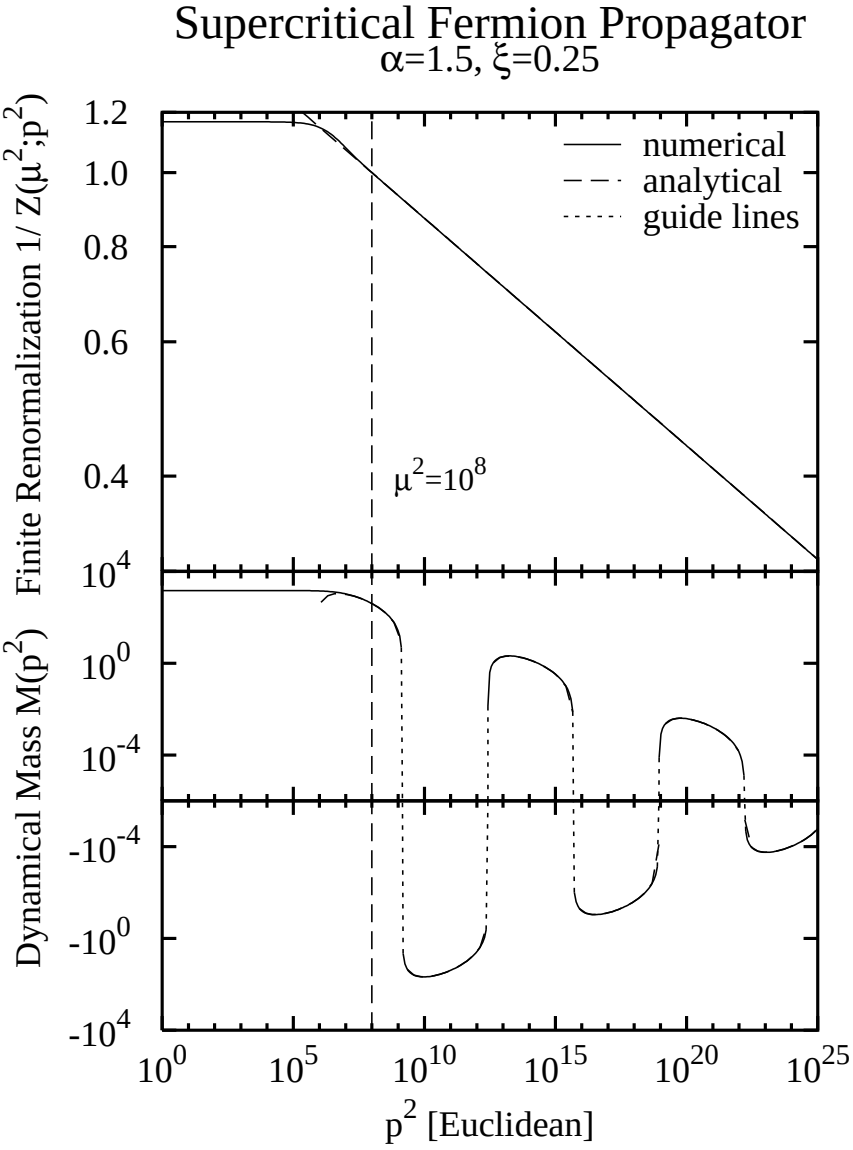

FIG. 3. Comparison of the numerical solution for the finite renormalization $1/Z(\mu^2; p^2)$, and the mass function $M(p^2)$ (solid lines) and their predicted asymptotic behaviour with matching scales (dashed lines) from Eqs. (3.8) and (3.13) for the supercritical coupling $\alpha = 1.5$. The example solution was for a renormalized mass $m_\mu = 400$ (arbitrary units), renormalization point $\mu^2 = 10^8$ and gauge parameter $\xi = 0.25$. The " guide lines" are added simply to guide the eye between data points on this logarithmic plot

TABLE I. This table compares the powers of the asymptotes of the finite renormalization and mass functions in Figs. 2 and 3, as determined analytically and by fitting the numerical solutions to a power law form.

Figure	coupling	determination	ν	$\mathrm{Re}\,(s)$	$\mathrm{Im}\,(s)$
2	$\alpha = 0.6$	analytical	0.01193662073	−0.181667015	
		numerical	0.01193662073	−0.181666808	
3	$\alpha = 1.5$	analytical	0.02984155182	−0.416012578	0.418128942
		numerical	0.02984155183	−0.416012521	0.418129001

C. Comparison of regularization schemes

We can now compare numerical solutions from the regularization-independent approach to those from cut-off regularization with the gauge-covariance modification [2], [5], [7] and those from dimensional regularization [8]. In cut-off regularization the fermion self-energies are integrated on a logarithmically spaced grid in k^2 momentum up to the highest (cut-off) momentum Λ^2. Additionally in dimensional regularization, an estimate is made of the contribution to the integral from the highest grid point to infinity. In both the modified cut-off and the dimensional regularization studies subtractive renormalization is performed numerically for the regularized (but otherwise divergent) fermion self-energies. For the modified UV cut-off regularization approach it was necessary to perform the calculation at several values of Λ and in principle perform a $\Lambda \to \infty$ extrapolation. In practice it was found that it was sufficient simply to ensure that Λ was chosen large enough. For the dimensional regularization approach it was necessary to calculate solutions at high accuracy for very many values of ϵ and then carefully extrapolate ϵ to 0. Numerical limitations made it difficult to obtain solutions at very small ϵ, which in turn limit the achievable accuracy of the $\epsilon \to 0$ extrapolation.

In Figs. 4 and 5, we compare these three regularization methods for subcritical ($\alpha = 0.6$) and supercritical ($\alpha = 1.5$) cases respectively, with the standard parameter choice of $\xi = 0.25$, $\mu^2 = 10^8$, $m_\mu = 400$. One can see the agreement between the regulator-independent (NR) and the modified cut-off and dimensionally regularized solutions is excellent. They are indistinguishable on the main figures: the inserts in Figs. 4 and 5 have the same p^2 scale and reveal the remarkable agreement between them in the infrared region. In Tables II and III we quantify the relative differences achieved between the three regularization schemes at a variety of momentum values. The difference between the results is entirely attributable to the limitations achievable in numerical precision. We can now conclude with some confidence that the three regularization schemes give identical results for the renormalized solutions.

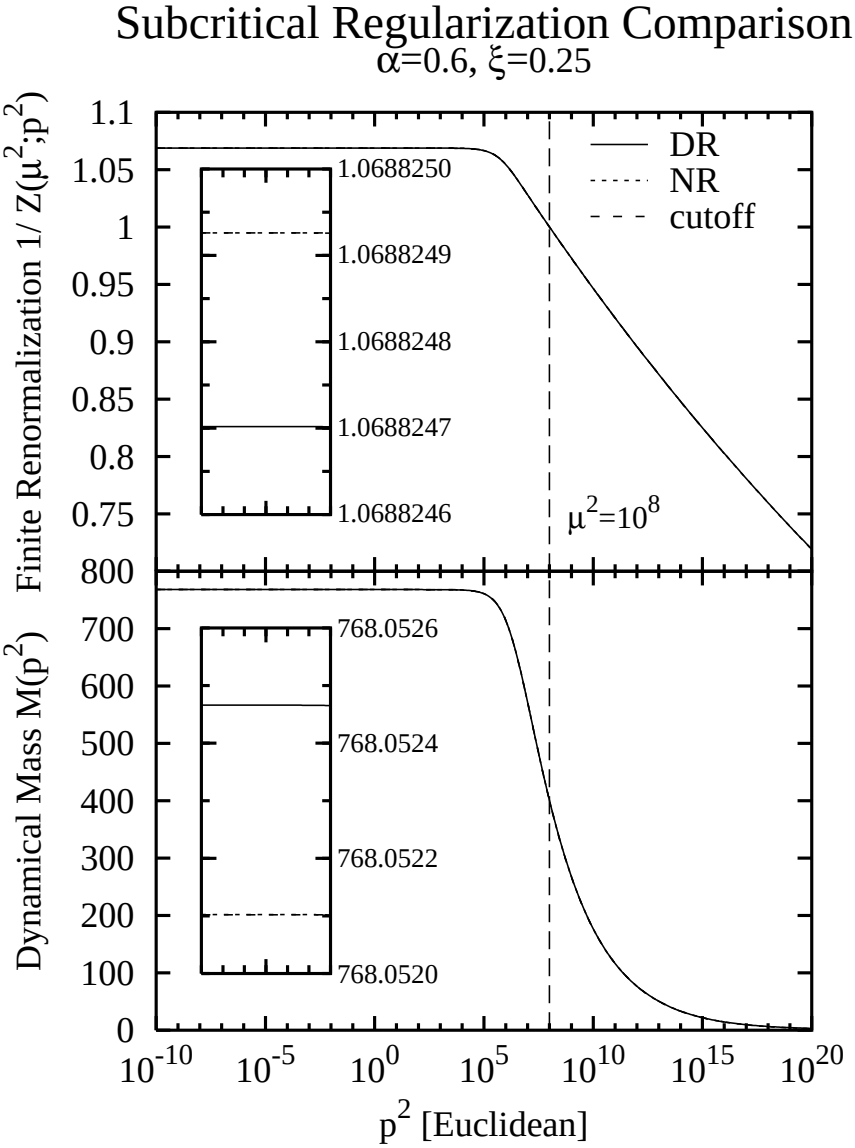

FIG. 4. The finite renormalization $1/Z(\mu^2;p^2)$ and dynamical mass $M(p^2)$ for the solution of the fermion SDE for subcritical coupling $\alpha = 0.6$ and gauge parameter $\xi = 0.25$ found from the regularization-independent (NR) method compared with solutions using the modified UV cut-off regulator and dimensional regularization. The dimensional regularization solution shown is the result of extrapolating various finite ϵ solutions at scale 10^3 to $\epsilon = 0$ using a fit cubic in ϵ at each momentum point. All solutions have renormalized mass $m_\mu = 400$ (in arbitrary units) at the renormalization point $\mu^2 = 10^8$. The small variation between the three regularization schemes is entirely attributable to limitations achievable in numerical precision.

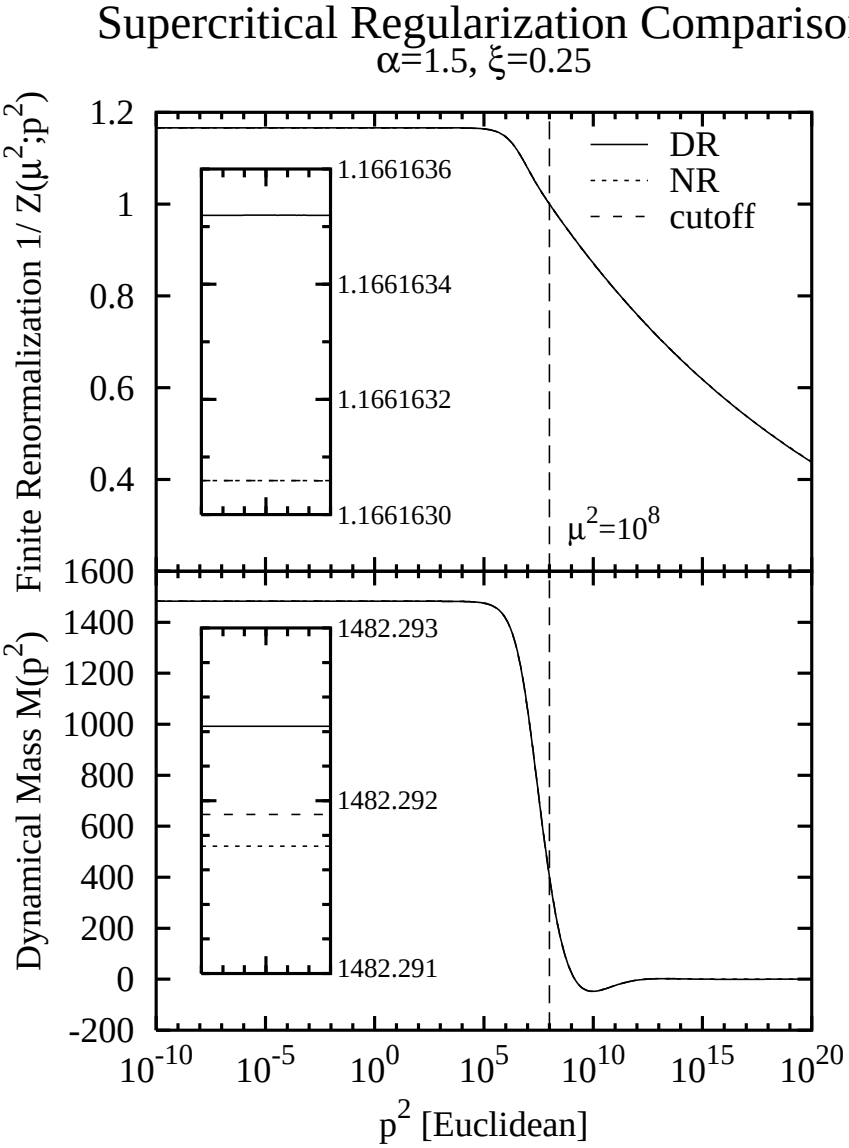

FIG. 5. The finite renormalization $1/Z(\mu^2;p^2)$ and dynamical mass $M(p^2)$ for the solution of the fermion SDE for supercritical coupling $\alpha = 1.5$ and gauge parameter $\xi = 0.25$ found from the regularization-independent (NR) method compared with solutions using the modified UV cut-off regulator and dimensional regularization. The dimensional regularization solution shown is the result of extrapolating various finite ϵ solutions at scale 10^3 to $\epsilon = 0$ using a fit cubic in ϵ at each momentum point. All solutions have renormalized mass $m_\mu = 400$ (in arbitrary units) at the renormalization point $\mu^2 = 10^8$. The small variation between the three regularization schemes is entirely attributable to limitations achievable in numerical precision.

TABLE II. This table shows the relative differences achieved for the finite renormalization $1/Z(\mu^2;p^2)$ between the regularization-independent approach and the modified UV cut-off and dimensional regularization (for cubic and quartic fits) approaches. The differences are averages over all momentum points solved in each order of magnitude shown. The solution parameters are the same as those in Figs. 4 and 5.

	reg. indp. vs.	$p^2=10^{-6}$	$p^2=10^{-2}$	$p^2=10^{2}$	$p^2=10^{6}$	$p^2=10^{10}$
$\alpha=0.6$	mod. cut-off	1.44×10^{-10}	1.45×10^{-10}	1.94×10^{-10}	5.35×10^{-8}	8.22×10^{-8}
	dim. reg. (cubic)	2.10×10^{-7}	2.10×10^{-7}	2.09×10^{-7}	9.05×10^{-8}	1.63×10^{-6}
	dim. reg. (quartic)	9.65×10^{-8}	9.64×10^{-8}	9.63×10^{-8}	6.11×10^{-8}	1.13×10^{-7}
$\alpha=1.5$	mod. cut-off	1.32×10^{-10}	1.73×10^{-10}	4.82×10^{-9}	4.97×10^{-8}	2.05×10^{-7}
	dim. reg. (cubic)	3.95×10^{-7}	3.95×10^{-7}	2.13×10^{-7}	2.23×10^{-7}	3.64×10^{-6}
	dim. reg. (quartic)	2.04×10^{-6}	2.04×10^{-6}	5.73×10^{-7}	1.27×10^{-7}	6.92×10^{-7}

TABLE III. This table shows the relative differences achieved for the mass function $M(p^2)$ between the regularization-independent approach and the modified UV cut-off and dimensional regularization approaches. The parameters are the same as those in Figs. 4 and 5.

	reg. indp. vs.	$p^2=10^{-6}$	$p^2=10^{-2}$	$p^2=10^{2}$	$p^2=10^{6}$	$p^2=10^{10}$
$\alpha=0.6$	mod. cut-off	2.63×10^{-10}	2.63×10^{-10}	3.19×10^{-10}	3.51×10^{-7}	1.58×10^{-6}
	dim. reg. (cubic)	4.73×10^{-7}	4.73×10^{-7}	4.73×10^{-7}	4.52×10^{-7}	2.34×10^{-5}
	dim. reg. (quartic)	5.16×10^{-7}	5.16×10^{-7}	5.16×10^{-7}	9.88×10^{-7}	4.18×10^{-6}
$\alpha=1.5$	mod. cut-off	1.24×10^{-7}	1.24×10^{-7}	1.23×10^{-7}	2.57×10^{-7}	6.47×10^{-5}
	dim. reg. (cubic)	4.68×10^{-7}	4.68×10^{-7}	9.29×10^{-7}	1.08×10^{-6}	2.06×10^{-4}
	dim. reg. (quartic)	1.64×10^{-6}	1.64×10^{-6}	5.22×10^{-7}	4.26×10^{-7}	3.74×10^{-5}

IV. CONCLUSIONS AND OUTLOOK

In this paper we have for the first time solved the Schwinger-Dyson equations for the fermion propagator in quenched QED_4 using the regularization-independent approach recently proposed in Ref. [9]. This has been done for the particular choice of the Curtis-Pennington transverse photon-fermion vertex, since this facilitates comparison with previous results which used the (gauge-covariance) modified UV cut-off and the dimensional regularization schemes. We have carried out precise calculations in these three approaches and have achieved excellent numerical agreement between them. This clearly demonstrates that we are able to achieve high-precision non-perturbative calculations of the renormalized fermion propagator that are free from any spurious errors which might arise from the regularization procedure itself.

We have derived and used the asymptotic analytic form of the solutions to obtain high accuracy even at extremely large momentum scales ($\mathcal{O}(10^{65})$). The reason that this is possible now is because in the regularization-independent approach all momentum integrations are finite by construction, [see Eq. (2.11)]. No bare mass or renormalization constants appear

in this formulation, since they have been eliminated by combining and subracting renormalized quantities. Since contact with the bare theory is lost, the onset of dynamical chiral symmetry breaking is signalled by the onset of oscillations in the UV mass function. This is a well-studied phenomena in quenched QED_4. We have derived the explicit analytical forms for the oscillations in the asymptotic region above critical coupling, including the period and decay envelope of these.

The importance of this regularization-independent approach lies in the fact that since all unregularized momentum integrations are finite from the outset, we do not have the mixing of small and arbitrarily large momentum scales in the intermadiate stages of our numerical calculations. This means that we can achieve high accuracy for solutions in the low and medium momentum regime with great numerical economy. This new approach will now permit numerically tractable studies of *unquenched* QED_4. These studies are now underway.

ACKNOWLEDGMENTS

This work was supported by the Australian Research Council. We thank Andreas Schreiber for numerous helpful discussions.

APPENDIX A:

The expressions mentioned in section III are given below.
The Ball-Chiu vertex [15] is

$$\Gamma^{\mu}_{BC}(\mu;k,p) = \frac{1}{2}\left(\frac{1}{Z(\mu^2;k^2)}+\frac{1}{Z(\mu^2;p^2)}\right)\gamma^{\mu} + \frac{(k+p)^{\mu}}{k^2-p^2}\left[\left(\frac{1}{Z(\mu^2;k^2)}-\frac{1}{Z(\mu^2;p^2)}\right)\frac{(\not{k}+\not{p})}{2}-\left(\frac{M(k^2)}{Z(\mu^2;k^2)}-\frac{M(p^2)}{Z(\mu^2;p^2)}\right)\right] . \quad \text{(A1)}$$

The coefficient function of the transverse vertex (Curtis-Pennington) [14] is

$$\tau_6(\mu;k,p) = -\frac{1}{2\,d}\left(\frac{1}{Z(\mu^2;k^2)}-\frac{1}{Z(\mu^2;p^2)}\right) \quad ,$$

where

$$d = \frac{\left\{(k^2-p^2)^2+\left(M^2(k^2)+M^2(p^2)\right)^2\right\}}{(k^2+p^2)} \quad . \quad \text{(A2)}$$

The constituents of the integrand in Eqs. (3.2) and (3.3) are the renormalization-point independent kernel functions

$$I(k^2,p^2) = \frac{3}{2\,(k^2-p^2)}\left\{M(k^2)\left[M(k^2) - M(p^2)\,\frac{Z(\mu^2;k^2)}{Z(\mu^2;p^2)}\right]\right.$$

$$+\frac{1}{2}\frac{(k^2+p^2)\,(M^2(k^2)+M^2(p^2))^2}{\{(k^2-p^2)^2+(M^2(k^2)+M^2(p^2))^2\}}\left[1-\frac{Z(\mu^2;k^2)}{Z(\mu^2;p^2)}\right]\Bigg\}\left(\frac{k^4}{p^4}\,\theta(p^2-k^2)+\theta(k^2-p^2)\right)$$

$$+\xi\,\frac{Z(\mu^2;k^2)}{Z(\mu^2;p^2)}\,\frac{M(k^2)M(p^2)}{k^2}\,\left(\frac{k^4}{p^4}\,\theta(p^2-k^2)\right) \quad , \tag{A3}$$

$$J(k^2,p^2) = \frac{3}{2}\,M(k^2)\left\{1+\frac{Z(\mu^2;k^2)}{Z(\mu^2;p^2)}+\frac{(k^4-p^4)}{\{(k^2-p^2)^2+(M^2(k^2)+M^2(p^2))^2\}}\left(1-\frac{Z(\mu^2;k^2)}{Z(\mu^2;p^2)}\right)\right\}$$

$$\times\ \left(\frac{k^2}{p^2}\,\theta(p^2-k^2)+\theta(k^2-p^2)\right)$$

$$-\frac{3}{2}\,p^2\,\frac{Z(\mu^2;k^2)}{Z(\mu^2;p^2)}\frac{M(k^2)-M(p^2))}{k^2-p^2}\,\left(\frac{k^4}{p^4}\,\theta(p^2-k^2)+\theta(k^2-p^2)\right)$$

$$+\,\xi\,\frac{Z(\mu^2;k^2)}{Z(\mu^2;p^2)}M(k^2)\left(\frac{k^2}{p^2}\,\theta(p^2-k^2)\right) \quad . \tag{A4}$$

Linearizing Eqs. (A3) and (A4) in terms of the mass function yields

$$I(k^2,p^2) \quad \underset{k^2,p^2\gg M^2}{\longrightarrow} \quad I'(k^2,p^2)\equiv 0 \quad ,$$

$$J(k^2,p^2) \quad \underset{k^2,p^2\gg M^2}{\longrightarrow} \quad J'(k^2,p^2) \quad ,$$

where

$$\begin{aligned} J'(k^2,p^2) \quad &= \quad \xi\,\frac{1}{p^2}\,\frac{Z(\mu^2;k^2)}{Z(\mu^2;p^2)}\,M(k^2)\,\theta(p^2-k^2) \\ &+ \quad \frac{3}{2}\left\{\frac{2\,M(k^2)}{(p^2-k^2)}\,\left[p^2\frac{Z(\mu^2;k^2)}{Z(\mu^2;p^2)}-k^2\right]\left[\frac{\theta(p^2-k^2)}{p^2}+\frac{\theta(k^2-p^2)}{k^2}\right]\right. \\ &- \quad \left.\frac{Z(\mu^2;k^2)}{Z(\mu^2;p^2)}\frac{M(p^2)-M(k^2)}{(p^2-k^2)}\,\left[\frac{k^2}{p^2}\,\theta(p^2-k^2)+\frac{p^2}{k^2}\,\theta(k^2-p^2)\right]\right\} \ . \end{aligned} \tag{A5}$$

APPENDIX B:

This appendix is devoted to the analytic calculation of the wave-function renormalization and mass functions in the asymptotic limit. The quantities that we need to evaluate are

$$Z_{\rm high}(\mu^2;k_m^2,p^2) \equiv \frac{1}{Z(\mu^2,k_m^2)}\frac{\alpha}{4\,\pi}\,\int_{k_m^2}^{\infty}\frac{dk^2}{k^2+M^2(k^2)}\,\left[Z(\mu^2;p^2)\,I(k^2,p^2)-I(k^2,\mu^2)\right]$$

$$M_{\rm high}(\mu^2;k_m^2,p^2) \equiv \frac{1}{M(k_m^2)}\frac{\alpha}{4\,\pi}\int_{k_m^2}^{\infty}\frac{dk^2}{k^2+M^2(k^2)} \times\Big[J(k^2,p^2)-J(k^2,\mu^2)+M(p^2)\,I(k^2,p^2)-m_\mu I(k^2,\mu^2)\Big] \tag{B1}$$

where $I(k^2,p^2)$ and $J(k^2,p^2)$ are given in appendix A. Provided k_m^2 is sufficiently large that $k_m^2 \gg M^2(k_m^2)$ then these quantities become

$$\int_{k_m^2}^{\infty}\frac{dk^2}{k^2+M^2(k^2)}\,I(k^2,p^2)\underset{k_m^2\gg M^2(k_m^2)}{=}\int_{k_m^2}^{\infty}\frac{dk^2}{k^2}\Bigg\{-\frac{3}{2}\,\frac{M(p^2)\,M(k^2)}{(k^2-p^2)}\,\frac{Z(\mu^2;k^2)}{Z(\mu^2;p^2)} +\frac{3}{4}\,M^4(p^2)\,\frac{(p^2+k^2)}{(k^2-p^2)^3}\left(1-\frac{Z(\mu^2;k^2)}{Z(\mu^2;p^2)}\right)\Bigg\}$$

$$\int_{k_m^2}^{\infty}\frac{dk^2}{k^2+M^2(k^2)}\,J(k^2,p^2)\underset{k_m^2\gg M^2(k_m^2)}{=}\int_{k_m^2}^{\infty}\frac{dk^2}{k^2}\Bigg\{3\,M(k^2)+3\,M(k^2)\,\frac{p^2}{(k^2-p^2)}\left(1-\frac{Z(\mu^2;k^2)}{Z(\mu^2;p^2)}\right) -\frac{3}{2}\,p^2\,\frac{Z(\mu^2;k^2)}{Z(\mu^2;p^2)}\,\frac{M(k^2)-M(p^2)}{(k^2-p^2)}\Bigg\} \tag{B2}$$

We have already shown for $k^2 \gg M^2$ that the wave-function renormalization and the mass function have a power law behaviour

$$Z(\mu^2;k^2)=C_\mu\left(\frac{k^2}{\mu^2}\right)^{\nu} \qquad M(k^2)=\frac{1}{2}D_\mu\left(\frac{k^2}{\mu^2}\right)^{-s}+\frac{1}{2}D_\mu^*\left(\frac{k^2}{\mu^2}\right)^{-s^*}. \tag{B3}$$

The results for $Z_{\rm high}$ and $M_{\rm high}$ for large k_m^2 and arbitrary p^2 and μ^2 can then be given in terms of hypergeometric functions

$$\begin{aligned} Z_{\rm high}(\mu^2;k_m^2,p^2) &= \frac{3\,\alpha}{16\,\pi}\,\Big[Z(\mu^2;p^2)\,\tilde I(p^2)-\tilde I(\mu^2)\Big] \\ M_{\rm high}(\mu^2;k_m^2,p^2) &= \frac{3\alpha}{8\,\pi}\,\Big[\tilde J(p^2)-\tilde J(\mu^2)+M(p^2)\,\tilde I(p^2)-m_\mu\,\tilde I(\mu^2)\Big] \end{aligned} \tag{B4}$$

with

$$\begin{aligned} \tilde I(p^2)=\Bigg\{ & M^4(p^2)\left[\frac{p^2}{3\,(k_m^2)^3}\,F(3,3,4,p^2/k_m^2)+\frac{1}{2\,(k_m^2)^2}\,F(3,2,3,p^2/k_m^2)\right] \\ & -\frac{M^4(p^2)}{Z(\mu^2;p^2)}\,\frac{C_\mu}{(\mu^2)^\nu}\Bigg[\frac{1}{(3-\nu)}\,\frac{p^2}{(k_m^2)^{3-\nu}}\,F(3,3-\nu,4-\nu,p^2/k_m^2) \\ & \qquad +\frac{1}{(2-\nu)}\,\frac{1}{(k_m^2)^{2-\nu}}\,F(3,2-\nu,3-\nu,p^2/k_m^2)\Bigg] \\ & +\frac{M(p^2)}{Z(\mu^2;p^2)}\,\frac{C_\mu\,D_\mu}{(\mu^2)^{\nu-s}}\,\frac{(k_m^2)^{\nu-s-1}}{(\nu-s-1)}\,F(1,1-\nu+s,2-\nu+s,p^2/k_m^2) \\ & +\frac{M(p^2)}{Z(\mu^2;p^2)}\,\frac{C_\mu\,D_\mu^*}{(\mu^2)^{\nu-s^*}}\,\frac{(k_m^2)^{\nu-s^*-1}}{(\nu-s^*-1)}\,F(1,1-\nu+s^*,2-\nu+s^*,p^2/k_m^2)\Bigg\}, \end{aligned} \tag{B5}$$

and

$$\tilde{J}(p^2) = \Bigg\{ \quad \frac{D_\mu}{(\mu^2)^{-s}} \, \frac{p^2}{(1+s)\,(k_m^2)^{s+1}} \; F(1, 1+s, 2+s, p^2/k_m^2)$$
$$+ \frac{D_\mu^*}{(\mu^2)^{-s^*}} \, \frac{p^2}{(1+s^*)\,(k_m^2)^{s^*+1}} \; F(1, 1+s^*, 2+s^*, p^2/k_m^2)$$
$$- \frac{3}{2} \, \frac{C_\mu \, D_\mu}{(\mu^2)^{\nu-s} \, Z(\mu^2; p^2)} \, \frac{p^2}{(1+s-\nu)\,(k_m^2)^{s-\nu+1}} \; F(1, 1+s-\nu, 2+s-\nu, p^2/k_m^2)$$
$$- \frac{3}{2} \, \frac{C_\mu \, D_\mu^*}{(\mu^2)^{\nu-s^*} \, Z(\mu^2; p^2)} \, \frac{p^2}{(1+s^*-\nu)\,(k_m^2)^{s^*-\nu+1}} \; F(1, 1+s^*-\nu, 2+s^*-\nu, p^2/k_m^2)$$
$$- \frac{C_\mu}{(\mu^2)^{\nu}} \, \frac{M(p^2)}{Z(\mu^2; p^2)} \, \frac{p^2}{(\nu-1)\,(k_m^2)^{\nu-1}} \, F(1, 1-\nu, 2-\nu, p^2/k_m^2) \Bigg\} . \tag{B6}$$

REFERENCES

[1] C.D. Roberts and A.G. Williams, Prog. Part. Nuc. Phys. **33** (1994) 477.
[2] F.T. Hawes and A.G. Williams, Phys. Rev. D **51** (1995) 3081 and references therein.
[3] Z. Dong, H. Munczek, and C. D. Roberts, Phys. Lett. **333B** (1994) 536.
[4] D.C. Curtis and M.R. Pennington, Phys. Rev. D **42** (1990) 4165 and references therein.
[5] F.T. Hawes, A.G. Williams and C.D. Roberts, Phys. Rev. D **54** (1996) 5361.
[6] A. Kızılersü, T. Sizer and A. G. Williams, ADP-99-43-T380, hep-ph/0001147.
[7] F.T. Hawes, T. Sizer and A.G. Williams, Phys. Rev. D **55** (1997) 3866.
[8] A.W. Schreiber, T. Sizer and A.G. Williams, Phys. Rev. D **58** (1998) 125014 ; V. P. Gusynin, A. W. Schreiber, T. Sizer and A.G. Williams, Phys. Rev. D **60** (1999) 065007.
[9] A.Kızılersü, A.W. Schreiber and A.G. Williams, ADP-0051/T431, hep-th/0010161 (to appear in Phys. Lett. B)
[10] D.C. Curtis and M.R. Pennington, Phys. Rev. D **46** (1992) 2663.
[11] V. A. Miransky, Phys. Lett. **165B** (1985) 401; *ibid*, Il Nuovo Cim. **90A** (1985) 149; see also D. Atkinson and P. W. Johnson, Phys. Rev.D **35** (1987) 1943.
[12] P. I. Fomin, V. P. Gusynin, V. A. Miransky and Yu. A. Sitenko, Riv. Nuovo Cim. **6** (1983) 1.
[13] V. A. Miransky, *Dynamical Symmetry Breaking in Quantum Field Theories*, (World Scientific, Singapore, 1993).
[14] D.C. Curtis and M.R. Pennington, Phys. Rev. D **42** (1990) 4165 and references therein.
[15] J.S. Ball and T.W. Chiu, Phys. Rev. D **22** (1980) 2512.
[16] D. Atkinson et al., Phys. Lett. **329B** (1994) 117.